Ligand-induced Changes in the Location of Actin, Myosin, 95K (α-Actinin), and 120K Protein in Amebae of *Dictyostelium discoideum*

JOAN M. CARBONI and JOHN S. CONDEELIS
Department of Anatomy and Structural Biology, Albert Einstein College of Medicine, Bronx, New York 10461

ABSTRACT In this study we investigated concanavalin A (Con A) induced changes in the locations of actin, myosin, 120K, and 95K (α-actinin) to determine the extent to which actin and myosin are reorganized during capping and the roles that 120K and 95K might play in this reorganization. We observed the location of each protein by indirect immunofluorescence using affinity purified antibodies. Four morphological states were distinguished in vegetative *Dictyostelium* amebae: ameboid cells before Con A binding, patched cells, capped cells, and ameboid cells with caps.

The location of each protein was distinct in ameboid cells both before and after capping. Actin and 120K were found in the cell cortex usually associated with surface projections, and myosin and 95K were diffusely distributed. Myosin was excluded from surface projections in ameboid cells. During patching, all four proteins were localized below Con A patches. During capping, actin, myosin, and 95K protein moved with the Con A patches into the cap whereas 120K protein was excluded from the cap. During the late stages of cap formation actin and myosin were progressively lost from the cap, and 120K became concentrated in new actin-filled projections that formed away from the cap. However, 95K remained tightly associated with the cap. Poisoning cells with sodium azide inhibited capping but not patching of ligand. In azide-poisoned cells, myosin and 95K did not co-patch with Con A, whereas copatching of 120K and actin with Con A occurred as usual.

Our results support the hypothesis that capping is an actomyosin-mediated motile event that involves a sliding interaction between actin filaments, which are anchored through the membrane to ligand patches, and myosin in the cortex. They are also consistent with a role for 120K in the formation of surface projections by promoting growth and/or cross-linking of actin filaments within projections, and with a role for 95K in regulating actomyosin-mediated contractility, earlier proposals based on the in vitro properties of these two proteins (Condeelis, J., M. Vahey, J. M. Carboni, J. DeMey, S. Ogihara, 1984, *J. Cell Biol.*, 99:119s–126s).

Cells of the vegetative stage of *Dictyostelium discoideum* are characterized as ameboid by their ability to exhibit dramatic shape changes involving extension and retraction of protrusions from the cell surface, events usually associated with locomotion on a substrate but that also occur when cells are in suspension. Another form of motility associated with the cell surface is chemotaxis, a process that involves an interaction between an extracellular ligand and the cytoskeleton (14, 18, 42) and that occurs during normal morphogenesis of this organism. A third process, exemplary of cell surface motility, is the ligand-induced capping of cell surface receptors, which, in this organism, is correlated with the ligand-induced recruitment of actin and myosin to the plasma membrane under ligand-receptor complexes (7, 8).

Although the motile mechanisms underlying these processes are not understood, a common theme has emerged that involves the actin cytomatrix in generating the force for membrane-associated motility. The cytoplasmic region immediately subjacent to the plasma membrane, the cell cortex, has been identified as an actin-rich zone containing dense

THE JOURNAL OF CELL BIOLOGY · VOLUME 100 JUNE 1985 1884–1893

networks of microfilaments (2, 8, 21). Much of this actin is tightly associated with the cell membrane and will co-purify with it (7, 28, 38). Interactions between the barbed ends of actin-containing filaments and the plasma membrane of *Dictyostelium* amebae have been observed in the electron microscope (2). This is the interaction most commonly seen in various cell types. In addition to these, numerous interactions have been observed in *Dictyostelium* amebae, between the sides of actin filaments and the plasma membrane that are mediated by lateral bridges 17 nm long (2). These are reminiscent of the lateral bridges seen in the microvilli of intestinal epithelial cells (32). Biochemical studies have also identified lateral interactions between microfilaments and the plasma membrane of *Dictyostelium discoideum* (22).

Finally, dramatic changes in the amount and organization of actin in the cell cortex occur during cell spreading (15, 34) and lectin binding and capping (7). Presumably, it is the growth and reorganization of actin filaments in the cell cortex, mediated by myosin and various actin binding proteins, that provide the force and spatial information necessary for changes in cell shape, locomotion, and capping. Hence, information about the location of actin and its associated proteins in these cells during ligand patching and capping is of considerable interest in the context of all forms of cell surface motility.

Myosin, 120K (9), and 95K (11, 16) are actin-associated proteins that are present in relatively large amounts in vegetative amebae and probably play important roles in the regulation of cortical actin structure. Both the 120K and 95K proteins have been characterized in detail (12). The 120K protein promotes the assembly of actin filaments and cross-links and branches actin filaments to form networks (8, 9, 12). It also inhibits the actin-stimulated Mg-ATPase of myosin. Previous work indicates that 120K is located in the cell cortex (10, 33). We have proposed that 120K protein participates in regulating the site of actin filament growth and gelation in vivo (12).

The 95K protein is *Dictyostelium* α-actinin: It cross-links actin filaments to form lateral arrays and stimulates, in a Ca^{2+}-dependent manner, the Mg-ATPase activity of actomyosin (12). It has been localized in the cell cortex and other regions of the cytoplasm (4). We have proposed that 95K helps organize actin filaments in vivo into lateral arrays suitable for interaction with myosin to produce force (12).

In this paper we describe the distribution in *Dictyostelium* amebae of actin, myosin, 120K, and 95K during various stages of patching and capping of the lectin concanavalin A (Con A)[1] on the cell surface, to determine the extent to which actin and myosin are reorganized in the cell cortex during capping and to infer the roles that 120K and 95K proteins might play in this reorganization.

MATERIALS AND METHODS

Preparation of Antigens: *Dictyostelium discoideum* strain AX-3 was grown in axenic culture (26) to a density of 1×10^7 cells/ml. *Dictyostelium* myosin was isolated according to previously published methods (31). The 120K protein was purified from *Dictyostelium* as described elsewhere (9).

Dictyostelium actin was isolated with modifications of the procedure of Gordon et al. (23) for the isolation of *Acanthamoeba* actin. The modifications are as follows: (*a*) The washed cell pellet was resuspended in 2 vol cold 5 mM Pipes (pH 7.0), 5 mM EGTA, 1 mM dithiothreitol, including 0.03 ml/ml Trasylol (Mobay Chemical Corp., Pittsburgh, PA) and 10 μg/ml Chymostatin (Sigmal Chemical Co., St. Louis) (2). Amebae were lysed in a Kontes glass homogenizer (Kontes Glass Co., Vineland, NJ) by hand (15–17 passes) at 0°C and the homogenate was centrifuged at 100,000 *g* for 1 h at 4°C. The supernatant was fractionated by passage over a DE52 column that had been saturated with ATP, and the actin, recovered from this column, was further purified according to Gordon et al. (23).

Dictyostelium 95K was isolated with modifications of the procedure of Condeelis and Vahey (11). The initial procedure for isolation of 95K protein is identical to that followed for actin isolation. The 95K protein elutes with actin between 0.17 and 0.27 M KCl. These fractions were pooled, made 2 mM in $MgSO_4$ from a 1 M stock, and incubated for 15 min at 22°C. Since Ca^{2+} and pH 7.6 inhibit the binding of 95K to F-actin (11), the incubation buffer was made 0.1 mM in $CaCl_2$ and pH 7.6, and F-actin was pelleted at 35,000 rpm for 3 h at 4°C. 95K protein was recovered in the supernatant, F-actin in the pellet. The supernatant was dialyzed overnight against two changes of 10 mM Pipes, 50 mM KCl, 0.5 mM EDTA, 0.25 mM dithiothreitol, pH 7.0. The dialyzed material was pumped onto a 1 × 30 cm column of Bio-Rad hydroxylapatite (Bio-Rad Laboratories, Richmond, CA) equilibrated in the above buffer, and 1 column vol of this buffer was passed through the column. The protein was eluted with a 400 ml gradient from 0 to 0.15 M potassium phosphate, pH 7.0. The position of 95K protein was detected by SDS PAGE. These fractions were pooled and dialyzed against 50 vol of the hydroxylapatite column buffer, and pumped onto a 1 × 2.5 cm column of hydroxylapatite. Bound protein was eluted with a 7-ml pulse of 100 mM potassium phosphate, pH 7.0. SDS PAGE was used to locate the purified protein.

Preparation of Antibodies: Preimmune sera were collected from New Zealand white rabbits and screened by Western blot analysis against homogenates of *Dictyostelium* amebae. Rabbits that showed no reaction against *Dictyostelium* antigens were injected with the purified antigens in complete Freund's adjuvant (1:1 vol/vol) subcutaneously along their dorsal surfaces. 0.5 mg of actin, myosin, 95K, and 120K, were injected at each inoculation. 3–4 wk later, each rabbit was boosted with 1 mg of the respective antigen in incomplete Freund's adjuvant between previously injected areas along the dorsal surface. 2 wk later rabbits were bled by cardiac puncture. Whole blood was allowed to clot at room temperature for 1 h and then at 4°C for 1 h. Separation of immune serum from the clot was achieved by centrifugation at 2,000 rpm for 10 min. Centrifugation was repeated until the serum was depleted of residual erythrocytes.

Affinity Purification of Antibodies: Monospecific antibodies against actin, myosin, 95K, and 120K were obtained from immune sera by affinity chromatography using CNBr-activated Sepharose 4B (Pharmacia Fine Chemicals, Piscataway, NJ) columns to which the respective *Dictyostelium* antigens had been covalently attached. Specifically bound antibody was eluted from the column by rinsing with 0.1 M glycine-HCl buffer, pH 2.8. The eluted protein fractions were neutralized immediately by the addition of 0.1 M Tris-HCl buffer, pH 8.5 and dialyzed overnight on ice into Tris-buffered saline (20 mM Tris, 0.9% NaCl, pH 7.6).

The amount of affinity purified antibody was determined spectrophotometrically assuming an $A^{1\%}_{280\ nm}$ of 14.4. The fractions were aliquoted and stored at −70°C after the addition of 0.02% NaN_3 and 1% BSA.

Electrophoretic Procedure and Western Blot Analysis: *Dictyostelium* amebae were resuspended to a final concentration of 1×10^7 cells/ml in PDF buffer (20 mM KCl, 40 mM sodium phosphate, 0.7 mM $CaCl_2$, 2 mM $MgSO_4$, pH 6.4) containing 10 μg/ml Chymostatin and 0.04 ml/ml Trasylol. 400 μl of the cell suspension was added to 100 μl hot (5×) Laemmli sample buffer containing 30 mM dithiothreitol. The sample was boiled for 5 min and 90 μl was added to a single broad well (curtain) of a 5–15% polyacrylamide gradient gel.

SDS PAGE was carried out according to the procedure of Laemmli (25) in the microslab apparatus designed by Matsudaira and Burgess (30). Gels stained with Coomassie Blue were scanned with a Gilford spectrophotometer (Gilford Instrument Laboratories, Inc., Corning Glass Works, Oberlin, OH) at a wavelength of 650 nm. The area under the protein peaks was measured by cutting and weighing.

Electrophoretic transfer of proteins from unstained gels to nitrocellulose paper was done in a Hoefer Transphor Apparatus (Hoefer Scientific Instruments, San Francisco, CA) according to the techniques of Towbin et al. (41) in electrode buffer (20 mM Tris, 200 mM glycine, 0.05% Tween 20, 16% [vol/vol] methanol). Electrophoretic transfer was carried out exhaustively at 40 V for at least 24 h at 4°C. Dried, blocked strips were incubated with purified antibodies (0.2–2 μg) for 2 h and rinsed three times (15 min each) with 0.1% BSA-Tris-buffered saline, pH 8.2. The strips were then incubated with dilution of biotinylated goat anti-rabbit IgG secondary antibody (0.1% BSA-Tris-buffered saline, 1% fetal calf serum, pH 8.2) for 30 min. The strips were washed as above and incubated with a 1/50 dilution of the avidin-biotin-peroxidase complex (Vectastain Kit, Vector Laboratories, Inc., Burlingame, CA) in 0.1%

[1] *Abbreviation used in this paper:* Con A, concanavalin A.

BSA–Tris-buffered saline, pH 8.2. 4-Chloro-1 naphthal (3 mg/ml in methanol), diluted in 100 mM Tris–HCl, pH 7.6, and 0.8% hydrogen peroxide, was added to obtain a colored reaction product. The stained strips were photographed immediately upon drying.

Reagents: Fluorescein isothiocyanate was conjugated to Con A according to the procedure of Mallucci (29). For use in immunofluorescence experiments, a determined amount of lyophilized Con A was solubilized in SS buffer (10 mM sodium phosphate, 1 M NaCl, 0.25 mM $CaCl_2$, 0.25 mM $MnCl_2$, pH 7.0) overnight on ice and clarified at 9,500 rpm for 30 min. The supernatant was recovered and the protein concentration was determined spectrophotometrically under the assumption of an $A^{1\%}_{280\ nm}$ of 11.4.

Kinetics of Capping at 22°C: *Dictyostelium* amebae were resuspended in PDF buffer to 3×10^6/ml. Con A was added to cells in suspension to 70 μg/ml, and the cells were swirled on an orbital shaker at 22°C. Aliquots of cells were removed at 2, 10, 15, 20, 25, and 40 min after ligand challenge and immediately added to an equal volume of 7.4% formaldehyde while vortexing occurred. An aliquot of fixed cells was placed on a microscope slide, and a coverslip was placed over the drop of cells. The coverslip was sealed to the slide with clear nail polish, and the cells were viewed on a Zeiss Photomicroscope equipped with epi-illumination and filter sets for fluorescein.

Immunofluoresence Procedure: *Dictyostelium* amebae were washed and resuspended to 3×10^6/ml in PDF buffer and shaken at 22°C for 30 min. Before Con A was added an aliquot of cells was removed from suspension and added to an equal volume of 7.4% formaldehyde while vortexing occurred. Con A (70 μg/ml) was then added to the suspension of unfixed cells, and aliquots of cells were removed at various times after Con A challenge and fixed as before. 100 μl of fixed cells was added to a coverslip previously coated with 0.1% polyethylenimine, and the cells were allowed to adhere to the coverslip for 8 min. The coverslips were then washed twice for 5 min each time by immersion in small plastic beakers containing ~15 ml of room temperature PDF buffer. The coverslips were dipped briefly (5 s) in distilled H_2O and immediately added to a Coplin jar containing −20°C acetone. After 15 min the Coplin jar was submerged under distilled H_2O, and each coverslip was carefully moved into the H_2O and held there for ~30 s. By this procedure, air drying of cells, which sometimes caused collapse of very fine projections on the cell surface, was avoided after acetone permeabilization.

We carried out staining by removing each coverslip from the H_2O and inverting it onto 75 μl of blocking solution composed of 1% BSA–phosphate-buffered saline (PBS) (1% BSA, 10 mM sodium phosphate, 0.9% NaCl, pH 7.0) containing 1% FCS for 10 min in a humidified chamber. The coverslip was lifted away from the blocking solution, blotted, and immediately inverted onto 50 μl of antibody (20 μg/ml) diluted in 1% BSA–PBS, pH 7.0, for 1 h. It was then rinsed in two beakers, each containing 15 ml of 0.1% BSA–PBS, pH 7.0, for 5 min each. The coverslip was blotted and inverted onto 50 μl (1/1,000) rhodamine-labeled goat anti-rabbit IgG (Gibco Laboratories, Inc., Grand Island, NY) diluted in 1% BSA–PBS, pH 7.0, for 1 h. It was rinsed as above, blotted, and inverted onto a glass slide containing 25 μl of 0.1 M propyl gallate made in 50% glycerol–PBS, pH 7.0. The coverslips were sealed to glass slides with clear nail polish and stored at 4°C for future reference. Control experiments were performed as described above except for two modifications: (*a*) incubation of permeabilized cells with primary antibody alone, secondary antibody alone, primary antibody preabsorbed with native antigen overnight, or preimmune whole antisera followed by incubation with secondary antibody; or (*b*) unpermeabilized cells incubated with both primary and secondary antibodies. Cells were observed with either 40X or 100X Neoflur phase objectives on a Zeiss photomicroscope equipped with epi-illumination and standard filter sets for fluorescein and rhodamine. Images were recorded on Tri-X film and developed with Diafine (Eastman Kodak Co., Rochester, NY). Exposure times and printing conditions for both experimental and control preparations were identical.

Effect of Sodium Azide: *Dictyostelium* amebae were washed and resuspended in PDF buffer to 3×10^6 cells/ml as previously described. The cells were shaken for 15 min at 22°C and then incubated with 1 mM NaN_3 for 15 min more. Con A was added at 70 μg/ml for 2–45 min. The cells were fixed and stained as described above.

Percent Co-localization of Con A and the Antigens: We determined quantitatively the percent co-patching and co-capping of antigens with Con A on cells that had been fixed and stained according to the immunofluoresence procedure described above. Cells were counted as capped if more than half of the cell surface was cleared of Con A. Cells were counted as patched if punctate accumulations of Con A were seen on the cell membrane. Based on these criteria, an antigen was scored as co-patched if it was seen as a discreet "spot," i.e., was not diffuse, below Con A. An antigen was scored as co-capped if it was seen in the cap of Con A. Counts were made in a double blind format to determine the percent co-patching of ligand with antigen on cells that had been incubated with Con A and NaN_3.

RESULTS

Specificity of the Antibodies

Affinity-purified antibodies were used in the experiments described in this paper. We determined the specificity of these antibodies using nitrocellulose blots that had been prepared by exhaustive transfer of polypeptides from the original polyacrylamide gel (Fig. 1). When applied to blots of whole vegetative amebae previously separated by SDS PAGE, each antibody stained a band with the same mobility as that of the purified antigen. The two additional bands in the 120K whole cell blot (Fig. 1, lane *b*) are proteolytic fragments of 120K based on the following evidence: (*a*) polypeptides of 110K and 83K are the two most prominent fragments produced by limited proteolysis of 120K in vitro (9). The extra bands in Fig. 1, lane *b* comigrate with 110K and 83K. (*b*) The antiserum used as the source of the affinity purified anti-120K employed in this study has been demonstrated to be monospecific for 120K by immuno–double diffusion and immunoelectrophoresis (10). (*c*) The intensity of the two extra bands in whole cell blots stained with anti-120K varies depending upon the preparation. These bands are less intense when care is taken to avoid proteolysis during homogenization of the amebae as described above.

Control experiments were done to test further the specificity of the antibodies. Cells were stained by identical procedures for indirect immunofluorescence with affinity purified antibodies, preimmune sera, and affinity-purified antibodies preabsorbed with the corresponding purified antigen. As shown in Figs. 2 and 3, no staining was observed with any of the preimmune sera or antibodies preabsorbed with purified antigen, whereas cells stained with the affinity purified antibodies showed bright fluorescence (Figs. 4–8).

In addition, deletion of either the secondary antibody (rhodamine-conjugated goat anti–rabbit IgG) or permeabilization with acetone resulted in the absence of cell-associated fluorescence, demonstrating the lack of autofluorescence and the cytoplasmic location of the antigens, respectively (data not shown).

Immunofluorescence Localization

ACTIN: Before ligand is added, *Dictyostelium* amebae in suspension repeatedly extend and retract projections from their surfaces, resulting in extensive changes in cell shape. These projections stain intensely with anti-actin, and the

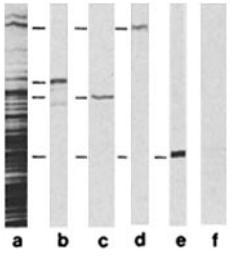

FIGURE 1 SDS PAGE and nitrocellulose blots of homogenates of *Dictyostelium* amebae. (a) SDS PAGE of homogenate of amebae stained with Coomassie Blue. (*b–e*) Nitrocellulose blots of a preparation identical to that in *a* stained with the following antibodies: (*b*) anti-120K, (*c*) anti-95K, (*d*) anti-myosin, and (e) anti-actin. Molecular masses of the bands indicated are, from top to bottom, 210,000, 120,000, 95,000 and 42,000. (*f*) A preparation identical to that in *a* after transfer of polypeptides to nitrocellulose. The gels in *a* and *f* were stained with Coomassie Blue by use of identical procedures to demonstrate that little stainable protein remains associated with the acrylamide gel after transfer to nitrocellulose and, hence, that the efficiency of transfer is high.

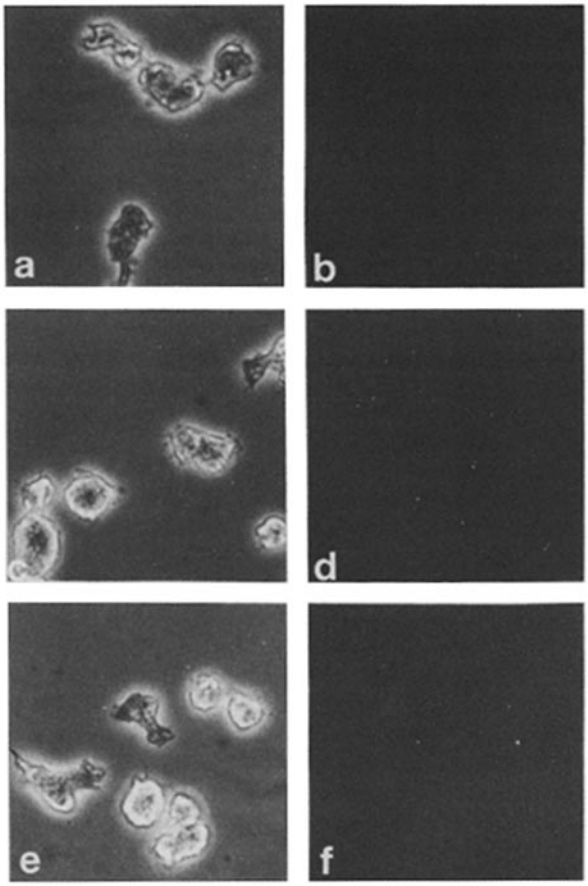

FIGURE 2 Staining of cells with preimmune serum. Cells were fixed and processed for immunofluorescence as usual except that preimmune serum at a dilution of 1/500 was substituted for the primary antibody. (*a*, *c*, and *e*) Phase and (*b*, *d*, and *f*) fluorescence images after staining with preimmune sera for (*b*) myosin, (*d*) actin, and (*f*) 95K. Exposures are identical to those in Figs. 3–8. × 625.

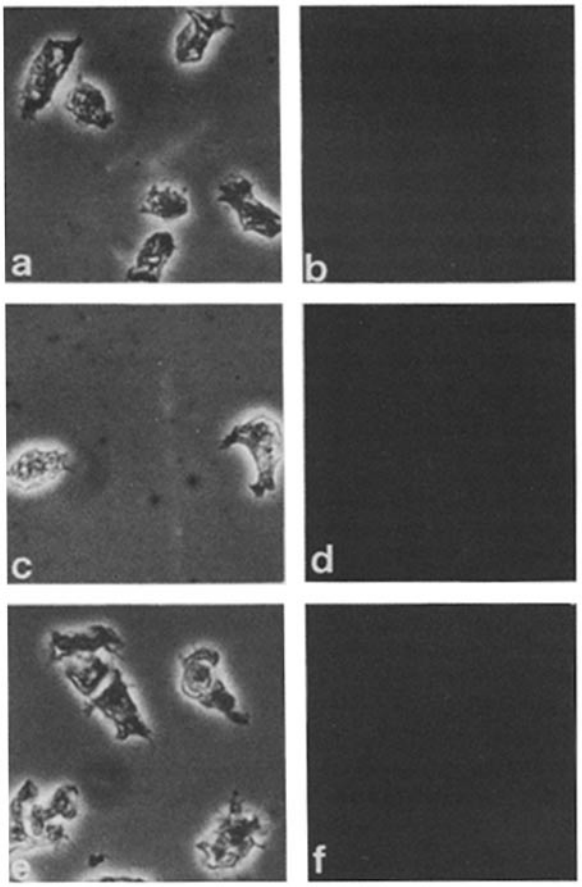

FIGURE 3 Staining of cells with affinity-purified antibodies after pre-absorption with purified antigen. Cells were fixed and processed for immunofluorescence as usual except that the affinity purified antibody was preincubated overnight with purified antigen (40 μg of antibody mixed with 300 μg antigen in 2 ml). (*a*, *c*, and *e*) Phase and (*b*, *d*, and *f*) fluorescence images after staining with (*b*) anti-myosin preabsorbed with myosin, (*d*) anti-actin preabsorbed with actin, and (*f*) anti-95K preabsorbed with 95K. × 625.

remainder of the cytoplasm shows relatively dim fluorescence (Fig. 4, *a–d*).

After the addition of Con A, amebae retract their projections and cease to extend new ones, so that after a few minutes the cells have rounded up (Fig. 4*e*). During this time (2–15 min after addition of Con A), Con A spontaneously forms patches on the cell surface. In such cells, actin is localized as a thin rim under the cell membrane and is often found to be concentrated under patches of Con A (Fig. 4, *e–g*).

If the cells are maintained in suspension at 22°C, they will move the patches of Con A into caps. The rate and extent of capping varies with the amount of Con A initially added to the cells. The results obtained with 70 μg/ml Con A as used in these experiments are shown in Fig. 5. During capping the anti-actin staining redistributes with the Con A patches into the cap (Fig. 4, *h–j*). Simultaneously, most cells extend new projections from their surfaces distant from the site where caps are forming. These new projections also stain with anti-actin (Fig. 4, *h–m*). Once capping is complete the cells exhibit the same dynamic extension and retraction of projections from their surfaces, as we observed before the addition of Con A, while the caps are eventually internalized. Intense anti-actin staining is progressively lost from the cap and becomes associated with the new surface projections (Fig. 4, *k–m*).

MYOSIN: Before Con A is added, myosin is localized in a patchy distribution throughout the cytoplasm but not in projections from the cell surface (Fig. 6, *a* and *b*). Hence, it is quite distinct from the distribution pattern observed for actin. However, upon addition of Con A, anti-myosin staining undergoes a dramatic redistribution into the cell cortex and is associated with Con A patches and caps (Fig. 6, *c–h*). Once a cap has formed, myosin staining is progressively lost from the cap, but, unlike actin, myosin becomes localized in a diffuse distribution throughout the cytoplasm as it was before Con A addition (Fig. 6, *i–k*) and is not associated with new projections that form away from the cap (Fig. 6, *l–n*).

95K PROTEIN: Before the addition of Con A, the distribution of 95K is distinct from that observed for either actin or myosin. Unlike actin, 95K is found in a patchy distribution throughout the cytoplasm, and, unlike myosin, it is also observed in some cell surface projections (Fig. 7, *a–d*). Addition of Con A causes a dramatic redistribution of anti-95K staining into the cell cortex where it is observed as a thin rim under the cell membrane and eventually becomes associated with Con A patches (Fig. 7, *e–j*). During capping, 95K redistributes with Con A patches into the cap, but, unlike the distribution found for either actin or myosin, distribution of 95K tends to remain associated with the cap even after capping is completed (Fig. 7, *k–m*).

120K PROTEIN: Before the addition of Con A, the dis-

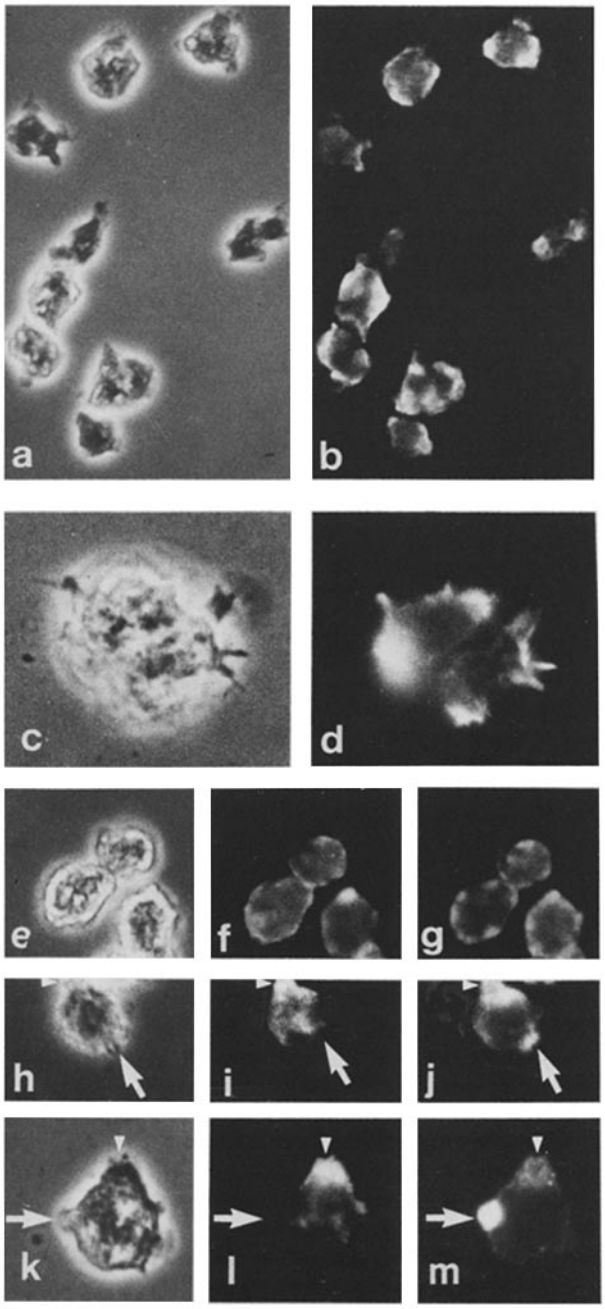

FIGURE 4 *Dictyostelium* amebae stained with anti-actin. *a*, *c*, *e*, *h*, and *k* are phase micrographs; *f*, *i*, and *l* show the distribution of Con A; and *b*, *d*, *g*, *j*, and *m* show fluorescence due to staining with anti-actin. (*a–d*) Before the addition of Con A, actin is associated with surface projections on amebae in suspension. (*e–g*) As Con-A patches on the cell surface, actin accumulates in cortical patches below Con A. (*h–j*) Actin is found in the forming cap (arrowheads) and in new projections that form on regions of the cell surface distant from the cap (arrows). (*k–m*) After capping is complete, intense anti-actin staining is no longer associated with the cap (arrowheads) but is now associated with surface projections which form at sites distant from the cap (arrows). (*a* and *b*) × 625. (*c* and *d*) × 1,700. (*e–g*) × 750. (*h–j*) × 1,000. (*k–m*) × 1,400.

tribution of the 120K resembles that found for actin: Staining for 120K is associated with the cell cortex and projections from the cell surface, whereas the remainder of the cytoplasm shows relatively dim fluorescence (Fig. 8, *a–d*). After the addition of Con A, 120K is found associated with Con A

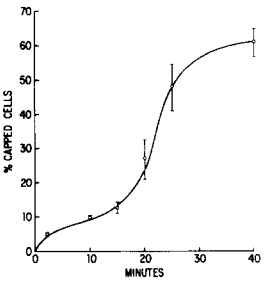

FIGURE 5 The capping of *Dictyostelium* amebae in suspension. The rate and extent of capping shown here are typical of the results obtained upon addition of 70 μg/ml of Con A to 3×10^6 cells/ml at 22°C. The error bars indicate the spread of data obtained for three experiments. 500 cells were counted.

patches (Fig. 8, *e–g*), but, unlike actin, myosin, and 95K, 120K is excluded from the cap (Fig. 8, *h–j*). During capping, 120K becomes localized in surface projections that form away from the cap (arrows, Fig. 8, *h–j*).

Percent Co-localization of Con A and the Antigens

Cells were scored for co-patching and co-capping of the various antigens with Con A as described above. At the times indicated in Fig. 9 all four antigens showed substantial co-patching with Con A, and this increased between 15 and 40 min. Scores for cells that were capped at 40 min demonstrate that actin, myosin, and 95K are present in most caps whereas 120K is conspicuously absent. These results confirm those shown in Figs. 4–8.

Effect of Sodium Azide on the Localization of the Antigens during Con A Patching

It has been well documented that movement of receptors into patches is energy independent, but capping requires metabolic energy (27, 39). Hence, it is possible to separate patching from capping with a metabolic poison such as sodium azide. By forcing the cells to accumulate in the patched state with sodium azide it is possible to score the co-localization of Con A and antigen with precision and determine if metabolic energy is required for accumulation of any of the antigens under the Con A patches.

Cells were incubated with 1 mM sodium azide for 15 min before the addition of Con A as described above. We then added Con A and allowed the cells to patch for 40 min before scoring them for co-localization of Con A patches and the antigens. The cells remained viable during this procedure as demonstrated by their ability to form caps and surface projections when sodium azide was removed by washing.

Figs. 10 and 11 summarize the effects of sodium azide on the co-localization of the antigens with patched Con A. In the presence of sodium azide, actin and 120K are localized to areas beneath the Con A patches as observed before in the absence of sodium azide. However, myosin and 95K are localized throughout the cytoplasm in the presence of sodium azide, and little co-localization is observed between these antigens and the patches of Con A. This contrasts sharply with the results obtained for myosin and 95K in the absence of sodium azide (Fig. 11).

To determine if the inhibition of co-localization of myosin, 95K, and Con A was due to an increase in the free Ca^{2+} concentration in the cytoplasm caused by sodium azide, 0.7 mM $CaCl_2$ in the incubation buffer was replaced with 0.1 mM EGTA, and the experiment was repeated. Double blind scoring of the co-localization of actin, myosin, 95K, and 120K with Con A demonstrated that identical results were obtained

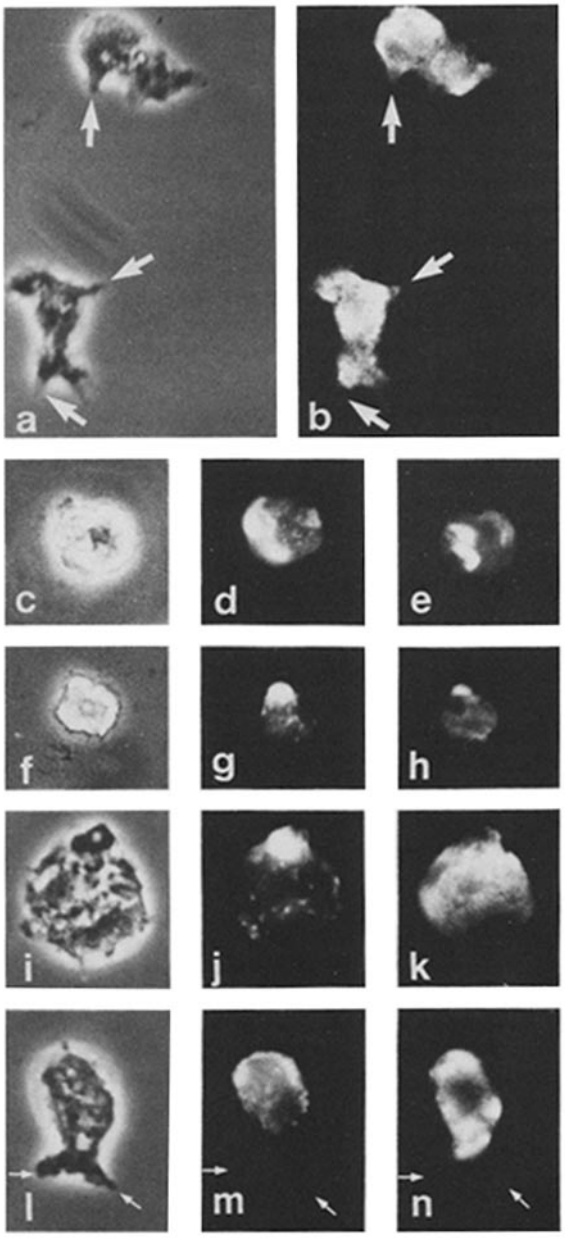

FIGURE 6 Amebae stained with anti-myosin. *a*, *c*, *f*, *i*, and *l* are phase micrographs; *d*, *g*, *j*, and *m* show the distribution of Con A; and *b*, *e*, *h*, *k*, and *n* show fluorescence due to staining with anti-myosin. (*a* and *b*) Before the addition of Con A, myosin is found in a diffuse distribution in the cytoplasm except for surface projections from which it is absent (arrows). After the addition of Con A, myosin is found in the cell cortex where it is co-patched (*c–e*) and co-capped (*f–h*) with Con A. (*i–k*) After capping is completed, anti-myosin staining of the cap is greatly diminished while most of the stain is found in a diffuse distribution in the cytoplasm. (*l–n*) New surface projections that form at sites away from the cap (arrows) do not stain for the presence of myosin. (*a* and *b*) × 625. (*c–h*) × 750. (*i–n*) × 1,400.

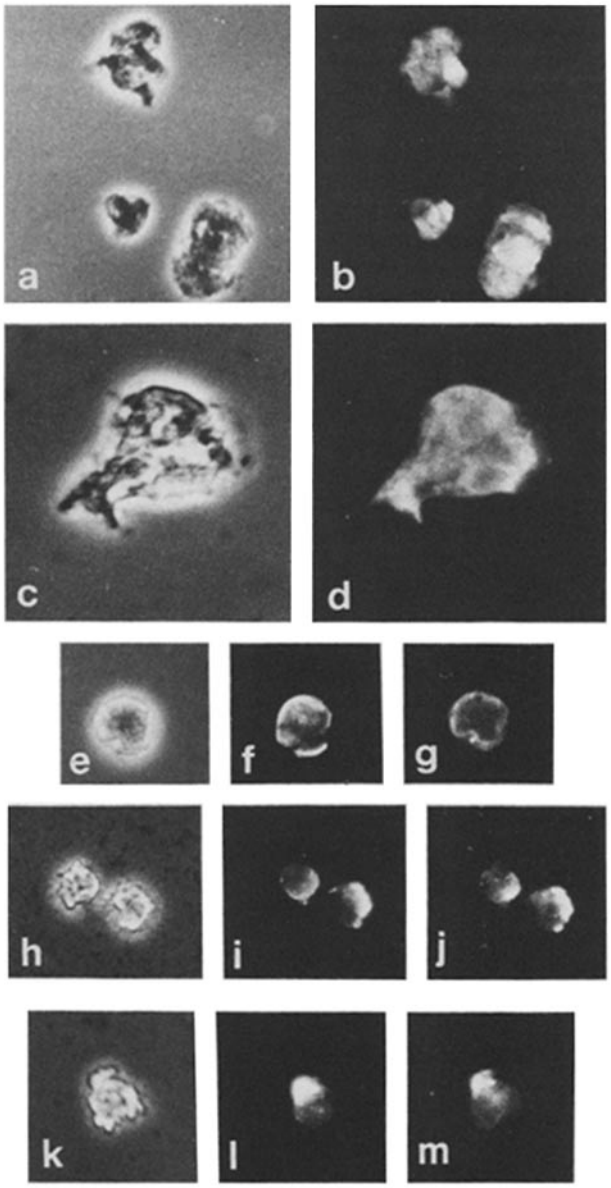

FIGURE 7 Amebae stained with anti-95K. (*a*, *c*, *e*, *h*, and *k*) are phase micrographs; *f*, *i*, and *l* show the distribution of Con A; and *b*, *d*, *g*, *j*, and *m* show fluorescence due to staining with anti-95K. (*a–d*) before the addition of Con A, 95K is found in a diffuse distribution in the cytoplasm, including surface projections. (*e–j*) When cells are patched, 95K undergoes a dramatic redistribution into the cell cortex where it underlies Con A patches. (*k–m*) Once capping is completed, 95K remains associated with the cap and is not found concentrated in other regions of the cytoplasm as are myosin and actin. (*a* and *b*) × 625. (*c* and *d*) × 1,700. (*e–m*) × 750.

whether $CaCl_2$ or EGTA was present in the extracellular medium.

DISCUSSION

The addition of Con A to *Dictyostelium* amebae in suspension causes a dramatic change in cell shape. A cell previously active in extension and retraction of projections from its surface will cease this activity and round up upon binding Con A. It will then actively cap patches of Con A that have passively formed on its surface. During the latter stages of capping the cell extends new projections from its surface usually away from where the cap has formed. Hence, four discrete morphological states can be distinguished: ameboid before Con A binding, patched, capped, and capped ameboid.

We conclude that the immunofluorescence pattern observed for each antigen in each morphological state is specific for several reasons. First, antibodies used in this study were affinity purified and demonstrated to be monospecific. Second, the immunofluorescence procedure used preserved fine

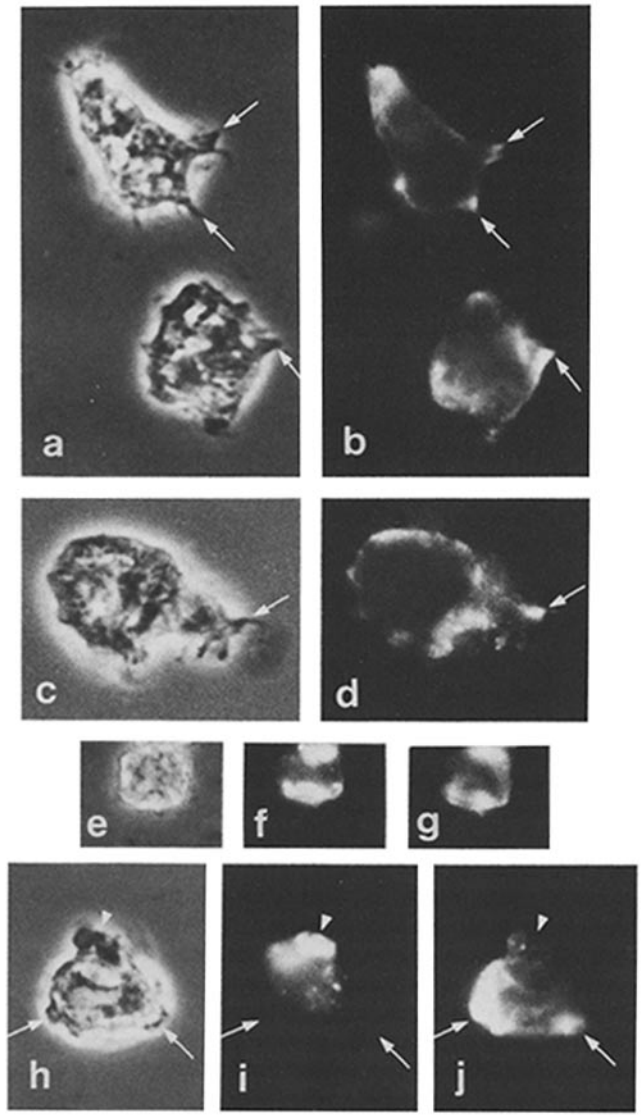

FIGURE 8 Amebae stained with anti-120K. *a*, *c*, *e* and *h* are phase micrographs; *f* and *i* show the distribution of Con A; and *b*, *d*, *g*, and *j* show fluorescence due to staining with anti-120K. (*a–d*) Before the addition of Con A, 120K is localized in the cell cortex and projections from the cell surface (arrows). (*e–g*) 120K is found to co-patch with Con A. (*h–j*) During capping, 120K is excluded from the cap (arrowhead). It is localized in surface projections that form at sites distant from the cap (arrows). (*a* and *b*) × 1,400. (*c* and *d*) × 1,700. (*e–g*) × 750. (*h–j*) × 1,400.

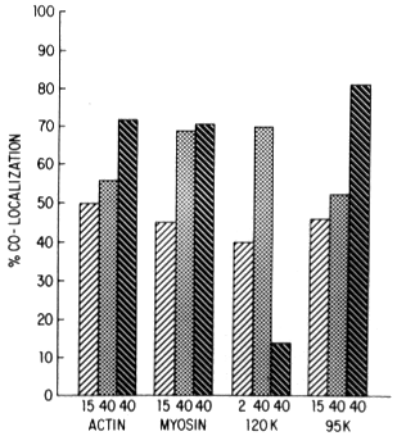

FIGURE 9 Percent co-localization of Con A and the antigens. Co-localization of each antigen with patches or caps of Con A was quantitated as described in Materials and Methods. Single lightly hatched and double hatched bars correspond to the percentage of patches of Con A that are co-patched with each antigen at the times indicated. Dense single hatched bars indicate the percentage of Con A caps that are co-capped with each antigen at 40 min. 100 cells were counted per bar.

structural features on the cell surface. Third, each antigen exhibited a distribution distinct from that of the other antigens in several of the four morphological states observed. Finally, the cortical distribution of actin and 120K in ameboid cells was not due to lack of accessible volume in the cytoplasm as suggested previously (4), since, in identical preparations, 95K and myosin showed a more diffuse cytoplasmic location, and myosin was excluded from cortical projections.

Significance of the Localization Patterns

ACTIN AND MYOSIN: Actin is the most abundant of the four proteins we studied. Estimates by densitometry indicate that of the total cell protein, actin constitutes ~8%; myosin, 2.3%; 120K, 2.3%; and 95K, 1.9% (12). In ameboid cells in suspension, both before and after capping, actin is found

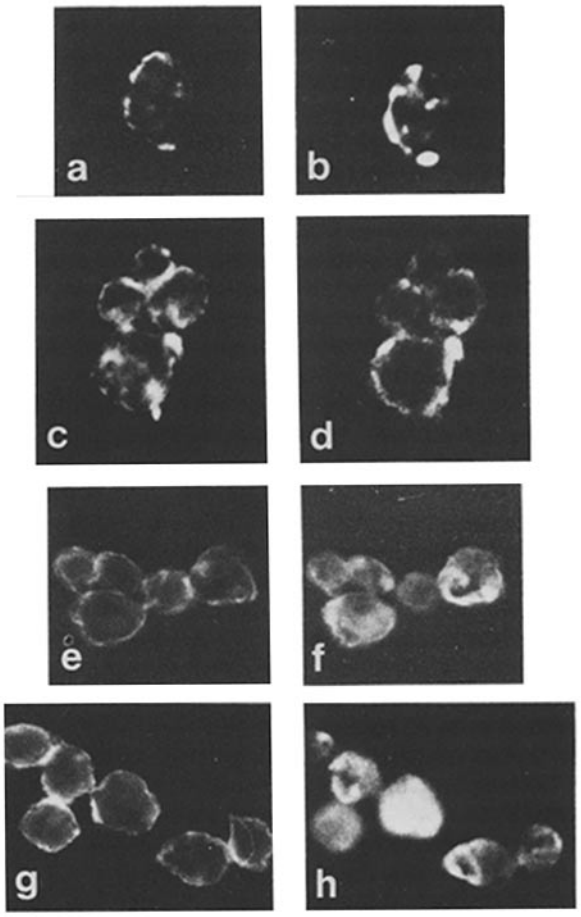

FIGURE 10 Effect of sodium azide on the localization of the antigens during Con A patching. a, *c*, *e*, and *g* show the location of Con A. *b*, *d*, *f*, and *h* demonstrate the location of the following antigens: (*b*) actin, (*d*) 120K, (*f*) 95K, and (*h*) myosin. Actin (*a* and *b*) and 120K (*c* and *d*) co-patch with Con A in the presence of NaN_3 whereas 95K (*e* and *f*) and myosin (*g* and *h*) remain diffusely distributed. × 700.

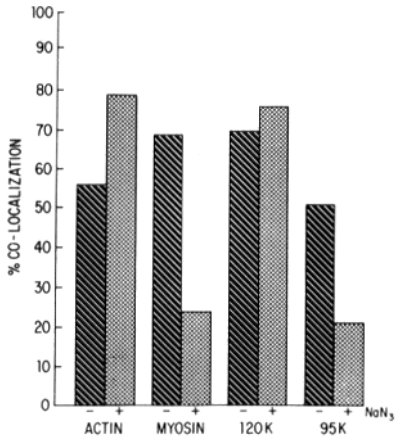

FIGURE 11 Percent co-localization of Con A patches and each antigen in the absence and presence of sodium azide. Single hatched bars indicate the percentage of Con A patches that are co-patched with each antigen at 40 min in the absence of NaN_3. Double hatched bars indicate the percentage of Con A patches that are co-patched with each antigen at 40 min in the presence of NaN_3. 100 cells were counted per bar.

concentrated in the cell cortex and its projections. This is the same distribution found in cells that have been permitted to spread and locomote on a surface (15, 34). The abundance and preponderance of this protein in cortical projections suggests that it might be involved in the growth and/or mechanical support of cell surface projections, functions analogous to the role of actin in the growth and maintenance of several well studied cell processess (13, 40).

The role that myosin might play in the growth of surface projections is not well understood. Although myosin is found distributed throughout the cytoplasm, it does not enter the projections (see reference 34 and Fig. 6). It has been suggested that myosin, located at the base of actin-containing projections, might play a role in mediating the translocation of F-actin within these structures, causing the projections to wag like a dog's tail (34).

Patching of Con A on the surface of ameboid cells in suspension causes recruitment of both actin and myosin into regions of the cell cortex below Con A patches. The redistribution of myosin is most dramatic since, unlike actin, which is already in the cell cortex, myosin must move from deeper in the cytoplasm into discrete locations in the cortex within minutes after Con A binding. This is consistent with the previous finding that plasma membranes isolated from cells during patching or capping of Con A contain ~20 times more myosin and three times more actin than do plasma membranes isolated from cells before Con A challenge (7).

Both actin and myosin move with Con A patches into the cap. This is the same result that has been reported for capping of a variety of ligands in cultured cells (19). Hence, our results further support the hypothesis that capping is an actomyosin-mediated motile event, as proposed previously for cultured cells (37) and *Dictyostelium* amebae (7).

During the final stages of capping, actin and myosin are progressively lost from the cap and return to other regions of the cytoplasm. A similar result has been observed for myosin in lymphocytes during IgG-induced capping (36). The newly recycled actin and myosin may be important for the resumption of ameboid movement that occurs at this time. This observation is consistent with a previous finding that the plasma membrane isolated from cells that had completed capping contains much less actin and myosin than does the plasma membrane isolated from patched cells (7). Possible physiological mechanisms for the dissociation of actin and myosin from the plasma membrane after capping are Ca^{2+} induced severing of actin filaments (2, 5, 21) and dissociation of myosin from the membrane by Mg–ATP (7).

120K: In vitro, 120K protein promotes the growth of actin filaments, cross-links filaments to form a gelled network, and inhibits the actin-stimulated Mg–ATPase of myosin. We have proposed that 120K helps determine the sites of actin filament growth and gelation in cells, resulting in gels that can expand their volume by polymerization of new actin filaments. Such gels could push on the plasma membrane to cause formation of projections at the cell surface (8, 12). Filaments within such a structure would be less able to activate the Mg–ATPase of myosin and participate in contractility. This hypothesis predicts that 120K should be found in situ in regions where actin polymerization and gelation, but not actomyosin-mediated contraction, are occurring.

The staining pattern obtained with anti-120K in ameboid cells in suspension resembles that for actin. It is associated with the cortex and, in particular, with projections of the cell surface. A similar type of distribution is observed in cells that have spread on a surface (10). Staining with rhodamine-labeled phallotoxin (34) and electron microscopy (2, 7, 8) showed cell surface projections to contain F-actin. The location of 120K in such projections may be sufficient to promote polymerization and/or to cross-link actin filaments, leading to the growth of these projections. Furthermore, the presence of 120k below Con A patches may be important for recruiting actin into this region. Studies employing high resolution immunocytochemistry are needed to study these possibilities further (33).

The ligand cap is a region where actin, myosin, and 95K have accumulated and, presumably, active contraction is occurring. The 120K protein, although present below Con A patches, is excluded from the cap. This is consistent with the prediction that 120K is unlikely to be found in regions of actomyosin mediated contractions. Exclusion could result from competition between myosin and 120K for actin binding (12).

95K: The 95K protein is *Dictyostelium* α-actinin (11, 12, 16). It cross-links actin filaments to form lateral arrays and stimulates, in a Ca^{2+}-dependent manner, the Mg–ATPase activity of actomyosin (12). We have proposed that in vivo, 95K helps to organize actin filaments into lateral arrays suitable for interaction with myosin to produce force (12). This hypothesis predicts that 95K should be found in situ where actomyosin is being assembled for contractility.

Cells in suspension show a distribution of 95K throughout the cytoplasm that is much less cortical than that observed in cells that have been spread on a surface (4). Binding of Con A to the cell surface causes dramatic recruitment of 95K into the cortex where it co-patches and co-caps with Con A. These results are reminiscent of the behavior of α-actinin in different types of vertebrate cultured cells during patching and capping of a variety of ligands (17, 20).

The sites of contractility within cells, whether in suspension or spread on a surface, are unknown, so the localization of 95K throughout the cytoplasm in ameboid cells before capping (Fig. 7 and reference 4) is not helpful in testing our hypothesis. This observation may indicate that any region of

the cytoplasm is capable of 95K-mediated assembly of actomyosin. However, the movement of 95K into patches and then the cap is consistent with the hypothesis, since in this situation 95K is associated with regions of the cell that contain actomyosin (7) that apears to be actively contracting.

It is possible that 95K, as an actin binding protein, is simply following the position of actin in the cell. If this were so, 95K should be cortical in ameboid cells even when in suspension, form co-patches with Con A in the presence of sodium azide, and rapidly vacate the cap after its formation to reside in new surface projections, since these are the locations of actin in identical preparations. However, 95K is distributed more diffusely in the first two cases and remains tightly capped in the latter.

Furthermore, previous work showed that cross-linking of surface receptors causes mobilization of Ca^{2+} from both extracellular (1, 35) and intracellular stores (3). It also causes the co-patching and capping of cytoplasmic calmodulin with the ligand, and this is believed to require a rise in cytoplasmic calcium levels (35). Therefore, the co-patching and capping of 95K with actin and myosin that we have shown here probably occur in the presence of elevated calcium levels. Since 95K would be dissociated from actin in the presence of calcium (11, 16), the position of 95K in the cell may reflect binding interactions between 95K and other proteins besides F-actin alone. We suspect that this interaction is between 95K and actomyosin, since 95K always co-localizes with actin when myosin does the same. We are currently investigating the possibility that 95K binds more strongly to actomyosin than to F-actin.

The Sodium Azide Effect

Incubation of cells with sodium azide causes reversible inhibition of electron transport in mitochondria (43), which is sufficient to inhibit capping in a variety of cell types (19). Patching of ligand still occurs as a result of passive diffusion and cross-linking of multivalent ligand-receptor complexes in the plane of the cell membrane (27). Our finding that 120K and actin become concentrated below Con A patches in the presence of sodium azide indicates that metabolic energy is not essential for the Con A–induced redistribution of these proteins. This is consistent with the observation that the interaction between 120K and actin in vitro is not influenced by ATP (9).

However, the presence of sodium azide blocks the Con A–induced redistribution of myosin and 95K into the cortex below Con A patches. It is not surprising that sodium azide affects the localization of myosin in situ. Variations in the ATP concentration caused by sodium azide could alter the degree of phosphorylation of the heavy chain of *Dictyostelium* myosin. This would produce a change in both the actin-stimulated Mg-ATPase of the myosin and the thick filament formation (24), either of which might alter the location of myosin in the cell. In fact, we will present experiments elsewhere to demonstrate that Con A and sodium azide affect the phosphorylated state of the myosin heavy chain in vivo (Carboni, J. M., and J. S. Condeelis, manuscript in preparation).

Sodium azide also inhibits the Con A–induced redistribution of 95K. It is possible that a decrease in cytoplasmic ATP concentration or oxidative phosphorylation would cause dissipation of pH and pCa gradients across plasma or cytoplasmic membranes. Since the binding of 95K to F-actin is inhibited at elevated pH and pCa (11, 16), a sodium azide–induced increase in either should inhibit the co-localization of actin and 95K in the cortex below Con A patches, if actin binding is the only mechanism involved in determining the location of 95K. Since varying the extracellular Ca^{2+} concentration in an acidic medium (pH 6.4) had no effect on the inhibition of 95K redistribution by sodium azide, dissipation of pH and pCa gradients across the plasma membrane are unlikely to be important in determining the distribution of 95K.

An alternative explanation for the inhibition of the Con A–induced redistribution of 95K by sodium azide is that 95K may have a higher affinity for actomyosin than for F-actin alone, as discussed above. Inhibition of the redistribution of myosin below Con A patches by sodium azide could decrease the affinity of 95K for actin in this domain. We are currently testing this possibility.

We acknowledge Dr. Edward Kuczmarski and Satoshi Ogihara for their helpful discussions, Dr. Patricia Detmers, Ms. Holly Bennett, and Mr. Rick Hock for their critical reading of the manuscript, and Ms. Edna Horowitz for her typing.

This study was supported by a grant from the National Institute of General Medical Sciences (25813) and a Hirschl Career Scientist Award.

This work was submitted in partial fulfillment of the requirements for the degree of Doctor of Philosophy (J. M. Carboni) and was presented in abstract at the 23rd Annual Meeting of The American Society for Cell Biology (6).

Received for publication 10 September 1984, and in revised form 31 January 1985.

REFERENCES

1. Allwood, G., G. L. Asherson, M. Davey, and P. J. Goodford. 1971. The early uptake of radioactive calcium by human lymphocytes treated with phytohaemagglutinin. *Immunology.* 21:509–516.
2. Bennett, H., and J. Condeelis. 1984. Decoration with myosin subfragment-1 disrupts contacts between microfilaments and the cell membrane in isolated *Dictyostelium* cortices. *J. Cell Biol.* 99:1434–1440.
3. Braun, J., R. I. Sha'afi, and E. R. Unanue. 1979. Crosslinking by ligands to surface immunoglobulin triggers mobilization of intracellular $^{45}Ca^{2+}$ in B lymphocytes. *J. Cell Biol.* 82:755–766.
4. Brier, J., M. Fechheimer, J. Swanson, and D. L. Taylor. 1983. Abundance, relative gelation activity, and distribution of the 95,000-dalton actin-binding protein from *Dictyostelium discoideum*. *J. Cell Biol.* 97:178–185.
5. Carboni, J. M. 1984. The cell cortex of *Dictyostelium discoideum*: a dynamic actin-containing compartment. Ph.D. thesis. Albert Einstein College of Medicine, New York. 137 pp.
6. Carboni, J. M., and J. S. Condeelis. 1983. Ligand induced changes in the structure of the actin cortex in *Dictyostelium discoideum*. *J. Cell Biol.* 97 (No. 5, Pt. 2):269a.
7. Condeelis, J. 1979. Isolation of concanavalin A caps during various stages of formation and their association with actin and myosin. *J. Cell Biol.* 80:751–758.
8. Condeelis, J. 1981. Microfilament-membrane interactions in cell shape and surface architecture. *In* International Cell Biology. *1980–81.* Springer-Verlag, Berlin. 306–320.
9. Condeelis, J., S. Geosits, and M. Vahey. 1982. Isolation of a new actin binding protein from *Dictyostelium discoideum*. *Cell Motil.* 2:273–285.
10. Condeelis, J., J. Salisbury, and K. Fujiwara. 1981. A new protein that gels F-actin in the cell cortex of *Dictyostelium discoideum*. *Nature (Lond.).* 292:161–163.
11. Condeelis, J., and M. Vahey. 1982. A calcium- and pH-regulated protein from *Dictyostelium discoideum* that cross-links actin filaments. *J. Cell Biol.* 94:466–471.
12. Condeelis, J., M. Vahey, J. M. Carboni, J. DeMey, and S. Ogihara. 1984. Properties of the 120,000 and 95,000 dalton actin-binding proteins from *Dictyostelium discoideum* and their possible functions in assembling the cytoplasmic matrix. *J. Cell Biol.* 99 (No. 1, Pt. 2):119s–126s.
13. Detmers, P. A., U. W. Goodenough, and J. Condeelis. 1983. Elongation of the fertilization tubule in *Chlamydomonas*: new observations on the core microfilaments and the effect of transient intracellular signals on their structural integrity. *J. Cell Biol.* 97:522–532.
14. Devreotes, P. N. 1982. Chemotaxis. *In* The Development of *Dictyostelium discoideum*, W. F. Loomis, editor. Academic Press, New York. 117–168.
15. Eckert, B. S., and E. Lazarides. 1978. Localization of actin in *Dictyostelium* amebas by immunofluorescence. *J. Cell Biol.* 77:714–721.
16. Fechheimer, M., J. Brier, M. Rockwell, E. Luna, and D. L. Taylor. 1982. A calcium- and pH-regulated actin binding protein from *D. discoideum*. *Cell Motil.* 2:287–308.
17. Feramisco, J. R., and S. H. Blose. 1980. Distribution of fluorescently labeled α-actinin in living and fixed fibroblasts. *J. Cell Biol.* 86:608–615.
18. Futrelle, R. P., J. Trout, and W. McKee. 1982. Cell behavior in *Dictyostelium discoideum*: preaggregation response to localized cyclic AMP pulses. *J. Cell Biol.* 92:807–821.
19. Geiger, B. 1983. Membrane-cytoskeleton interaction. *Biochim. Biophys. Acta.* 737:305–341.

20. Geiger, B., and S. J. Singer. 1979. The participation of α-actinin in the capping of cell membrane components. *Cell.* 16:213–222.
21. Giffard, R., J. A. Spudich, and A. Spudich. 1983. Ca^{2+}-sensitive isolation of a cortical actin matrix from *Dictyostelium* amoebae. *J. Muscle Res. Cell Motil.* 4:115–131.
22. Goodloe-Holland, C. M., and E. J. Luna. 1984. A membrane cytoskeleton from *Dictyostelium discoideum.* III. Plasma membrane fragments bind predominantly to the sides of actin filaments. *J. Cell Biol.* 99:71–78.
23. Gordon, D. J., E. Eisenberg, and E. Korn. 1976. Characterization of cytoplasmic actin isolated from *Acanthamoeba castellanii* by a new method. *J. Biol. Chem.* 251:4778–4786.
24. Kuczmarski, E. R., and J. A. Spudich. 1980. Regulation of myosin self-assembly: phosphorylation of *Dictyostelium* heavy chain inhibits formation of thick filaments. *Proc. Natl. Acad. Sci. USA.* 77:7292–7296.
26. Laemmli, U. K. 1970 Cleavage of structural proteins during the assembly of the head of bacteriophage T4. *Nature (Lond.).* 227:680–685.
26. Loomis, W. 1971. Sensitivity of *Dictyostelium discoideum* to nucleic acid analogues. *Exp. Cell Res.* 64:484–486.
27. Loor, F., L. Forni, and B. Pernis. 1972. The dynamic state of the lymphocyte membrane. Factors affecting the distribution and turnover of surface immunoglobulins. *Eur. J. Immunol.* 2:203–212.
28. Luna, E. J., V. M. Fowler, J. Swanson, D. Branton, and D. L. Taylor. 1981. A membrane cytoskeleton from *Dictyostelium discoideum.* I. Identification and partial characterization of an actin-binding activity. *J. Cell Biol.* 88:396–409.
29. Mallucci, L. 1976. *In* Concanavalin A as a Tool. H. Bitiger and H. P. Schnebli, editors. John Wiley & Sons, Inc., New York. 69–78.
30. Matsudaira, P. T., and D. R. Burgess. 1979. Identification and organization of the components in the isolated microvillus cytoskeleton. *J. Cell Biol.* 83:667–673.
31. Mockrin, S. C., and J. A. Spudich. 1976. Calcium control of actin-activated myosin adenosine triphosphatase from *Dictyostelium discoideum. Proc. Natl. Acad. Sci. USA.* 73:2321–2325.
32. Mooseker, M. S., and L. G. Tilney. 1975. The organization of an actin filament-membrane complex: filament polarity and membrane attachment in the microvilli of intestinal epithelial cells. *J. Cell Biol.* 67:725–743.
33. Ogihara, S., and J. Condeelis. 1983. Electron microscopic localization of myosin and 120K actin binding protein in the cortical actin matrix using IgG-gold. *J. Cell Biol.* 97 (No. 5, Pt. 2):270a.
34. Rubino, S., M. Fighetti, E. Unger, and P. Cappuccinelli. 1984. Location of actin, myosin and microtubular structures during directed locomotion of *Dictyostelium* amebae. *J. Cell Biol.* 98:382–390.
35. Salisbury, J. L., J. S. Condeelis, N. J. Maihle, and P. Satir. 1981. Calmodulin localization during capping and receptor-mediated endocytosis. *Nature (Lond.).* 294:163–166.
36. Schreiner, G. F., K. Fujiwara, T. D. Pollard, and E. R. Unanue, 1977. Redistribution of myosin accompanying capping of surface Ig. *J. Exp. Med.* 145:1393–1398.
37. Singer, S. J., J. F. Ash, L. Y. W. Bourguignon, M. H. Heggeness, and D. Louvard. 1978. Transmembrane interactions and the mechanisms of transport of proteins across membranes. *J. Supramol. Struct.* 9:373–389.
38. Spudich, J. 1974. Biochemical and structural studies of actomyosin-like proteins from non-muscle cells. II. Purification, properties and membrane association of actin from amoebae of *Dictyostelium discoideum. J. Biol. Chem.* 249:6013–6020.
39. Taylor, R. B., P. H. Duffus, M. C. Raff, and S. de Petris. 1971. Redistribution and pinocytosis of lymphocyte surface immunoglobulin molecules induced by anti-immunoglobulin antibody. *Nature (Lond.).* 233:225–229.
40. Tilney, L. G. 1978. Polymerization of actin. V. A new organelle, the actomere, that initiates the assembly of actin filaments in *Thyone* sperm. *J. Cell Biol.* 77:551–564.
41. Towbin, H., T. Staehelin, and J. Gordon. 1979. Electrophoretic transfer of proteins from polyacrylamide gels to nitrocellulose sheets: procedure and some applications. *Proc. Natl. Acad. Sci. USA.* 76:4350–4354.
42. Vicker, M. G., W. Schill, and K. Drescher. 1984. Chemoattraction and chemotaxis in *Dictyostelium discoideum*: *Myxamoeba* cannot read spatial gradients of cyclic adenosine monophosphate. *J. Cell Biol.* 98:2204–2214.
43. Wilson, D. F., and B. Chance. 1966. Reversal of azide inhibition by uncouplers. *Biochem. Biophys. Res. Commun.* 23:751–756.